RESEARCH ARTICLE | FEBRUARY 03 2016

First principles studies on the impact of point defects on the phase stability of $(Al_xCr_{1-x})_2O_3$ solid solutions

C. M. Koller ; N. Koutná ; J. Ramm ; S. Kolozsvári ; J. Paulitsch; D. Holec ; P. H. Mayrhofer

AIP Advances 6, 025002 (2016)
https://doi.org/10.1063/1.4941573

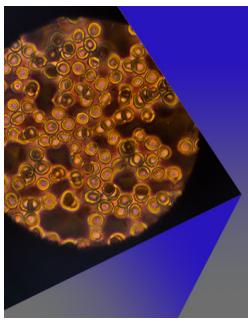

First principles studies on the impact of point defects on the phase stability of $(Al_xCr_{1-x})_2O_3$ solid solutions

C. M. Koller,[1,a] N. Koutná,[2] J. Ramm,[3] S. Kolozsvári,[4] J. Paulitsch,[1,6] D. Holec,[1,5] and P. H. Mayrhofer[1,6]

[1]*Christian Doppler Laboratory for Application Oriented Coating Development, TU Wien, Vienna, 1060, Austria*
[2]*Faculty of Science, Masaryk University, Kotlářská 2, Brno, 61137, Czech Republic*
[3]*Oerlikon Balzers, Oerlikon Surface Solutions AG, Balzers, 9496, Liechtenstein*
[4]*Plansee Composite Materials GmbH, Lechbruck am See, 86983, Germany*
[5]*Department of Physical Metallurgy and Materials Testing, Montanuniversität Leoben, Leoben, 8700, Austria*
[6]*Institute of Materials Science and Technology, TU Wien, Vienna, 1060, Austria*

(Received 15 May 2015; accepted 26 January 2016; published online 3 February 2016)

Density Functional Theory applying the generalised gradient approximation is used to study the phase stability of $(Al_xCr_{1-x})_2O_3$ solid solutions in the context of physical vapour deposition (PVD). Our results show that the energy of formation for the hexagonal α phase is lower than for the metastable cubic γ and B1-like phases–independent of the Al content x. Even though this suggests higher stability of the α phase, its synthesis by physical vapour deposition is difficult for temperatures below 800 °C. Aluminium oxide and Al-rich oxides typically exhibit a multi-phased, cubic-dominated structure. Using a model system of $(Al_{0.69}Cr_{0.31})_2O_3$ which experimentally yields larger fractions of the desired hexagonal α phase, we show that point defects strongly influence the energetic relationships. Since defects and in particular point defects, are unavoidably present in PVD coatings, they are important factors and can strongly influence the stability regions. We explicitly show that defects with low formation energies (e.g. metal Frenkel pairs) are strongly preferred in the cubic phases, hence a reasonable factor contributing to the observed thermodynamically anomalous phase composition. [http://dx.doi.org/10.1063/1.4941573]

I. INTRODUCTION

Increased productivity and the need to machine high temperature alloys require increased stability of cutting and forming tools. To some extent, this can be achieved by the application of physical vapour deposited, PVD, protective coatings. A prominent class of high performance coatings is represented by Al-based oxides which feature enhanced oxidation resistance as well as outstanding thermo–mechanical properties.[1,2] Solid solutions of $(Al_xCr_{1-x})_2O_3$ have gained high industrial attention, as Cr promotes the desired thermodynamically stable and mechanically resistant α phase (also known as the corundum structure).[3–6] However, it turns out that the low temperature growth of α-$(Al_xCr_{1-x})_2O_3$ by PVD techniques, as for instance magnetron sputter deposition or cathodic arc evaporation, is extremely challenging for higher Al-contents in the coating. Although α is the thermodynamically stable phase, coatings produced at typical PVD growth temperatures of ~550 °C usually contain also amorphous-like material or cubic oxide phases. Apart from the commonly known cubic-based Al_2O_3 polymorphs (e.g., γ-Al_2O_3) the presence of a metastable defected B1-like $(Al_xCr_{1-x})_2O_3$ solid solution was reported[7–10] and studied by *ab initio*.[11] Even though α-Al_2O_3 and its metastable polymorphs have been comprehensively investigated from both experimental and

[a]Corresponding author phone: +43 (1) 58801 308 100 mail: christian.martin.koller@tuwien.ac.at

computational aspects, only little is known about the new B1-like phase and its relation to α- and γ-type $(Al_xCr_{1-x})_2O_3$.

Based on previous studies it is well-known that substrate temperature and ion energies strongly affect film growth and properties.[12,13] Process temperatures higher than 800 °C increase the surface mobility of the adatoms, consequently providing the energy which is required for the stabilization of α-Al_2O_3.[14] However, there is a substantial interest to reduce the thermal load of the substrates during deposition and obtain crystalline α structured coatings at temperatures as low as 500 or 600 °C. Fundamental deposition processes such as the bombardment of atoms and ions not only provide energy to the growing film but also result in an increased distortion of the surface near region and the generation of multiple defects such as interstitials and vacancies,[15–17] in addition to dislocations etc. As defect annihilation requires mobility of the participating species, which is usually achieved by heating or by momentum transfer, conditions present at low temperature PVD are often not sufficient to overcome the energy barriers for diffusion. Consequently, the films exhibit increased defect densities. Ashenford et al.[18] examined phase stability trends of Al_2O_3 with respect to the influence of point defects using Molecular Dynamic and Monte Carlo methods. The initial defect concentration was suggested to play an essential role in a controlled α Al_2O_3 formation at temperatures below 500 °C. Music et al.[19] proposed that bombardment induced mobility enabled higher diffusion along the γ-Al_2O_3 (001) facets as compared with the α-Al_2O_3 (0001) plane and thus facilitated the growth of the latter. The important role of defects (e.g., point defects such as vacancies) in Al-based oxides can also be found in phase evolution studies of PVD processed oxynitrides,[20,21] where the formation of vacancies in the cubic Al-Cr-based oxynitride phase is necessary for maintaining the charge neutrality with increasing O/(N+O) ratio and, thus can also be related to the presence of a B1-like cubic phase in $(Al_{1-x}Cr_x)_2O_3$.

Defect formation energies predicted by *ab initio* methods have been demonstrated to be reasonably accurate for metals (with respect to experiments). However, the same treatment by Density Functional Theory (DFT)–applying conventional exchange correlation functionals (i.e. Local Density Approximation (LDA) or Generalised Gradient Approximation (GGA))–for ionic insulator materials turns out to be erroneous due to an underestimation of the band gap.[22] Similarly, other properties such as electronic levels of defect states or optical properties, are also predicted incorrectly. Therefore, huge efforts are being made to overcome these limitations in order not only to reproduce experimental results, but also to reliably predict properties.[23–25] In a recent review, Freysoldt et al.[26] comprehensively summarised the impact of point defects on material properties, including information on possible issues, drawbacks but also advantages of different methodical approaches (LDA+U,[27,28] hybrid functionals[29,30]). The progress can be demonstrated on an example of defect formation energies in α-Al_2O_3 by comparing literature published within the last decade.[31–35]

Research towards a reliable description of ionic insulating materials has been made rather slowly, only under huge efforts employing expensive non-standard methods. In almost all cases, experimental comparison is made with pure compounds, strongly contrasting with the present case of $(Al_xCr_{1-x})_2O_3$ solid solution thin films processed far from thermodynamic equilibrium and exhibiting high defect densities.

Including all the above mentioned improvements to address differences between the recently introduced B1-like structure, as well as the α and γ phases in the $(Al_xCr_{1-x})_2O_3$ system, would result in a tremendous complexity (ionic oxides, magnetism, alloying, defected structures), and is beyond the scope of the present work. Contrarily, our intention is to simplify the issue to a traceable problem, which, if successful, will serve as a basis for further more accurate studies.

We report on phase stability trends for the thermodynamically stable α and metastable cubic (γ and B1-like) $(Al_xCr_{1-x})_2O_3$ phases calculated by first principles methods. For the model system $(Al_{0.69}Cr_{0.31})_2O_3$ we have studied the impact of various point defects on the energy of formation of these cubic and hexagonal phases. Our results clearly suggest that point defects need to be considered to understand the experimentally observed phase evolution of $(Al_xCr_{1-x})_2O_3$ coatings, especially when prepared by PVD.

II. METHODOLOGY

Total energy calculations of the $(Al_{1-x}Cr_x)_2O_3$ system are performed using the Vienna Ab initio Simulation Package (VASP code),[36] a plane-wave implementation of the Density Functional Theory (DFT) in combination with pseudopotentials[37] using projector augmented wave method, generalized gradient approximation (GGA) for exchange-correlation effects by Perdew, Burke, and Ernzerhof.[38] A plane wave cut-off energy of 600 eV and a minimum of 1120 k-point · atoms (number of k-points is given in the whole Brillouin zone) ascertain accuracy in the order of $\sim 10^{-3}$ eV/atom. Supercells with 80 atoms for all three $(Al_xCr_{1-x})_2O_3$ phases–α (rhombohedral $R\bar{3}c$[39]), γ (fcc-based defect spinel $Fd\bar{3}m$[40–42]), and ordered vacancy phase B1-like, according to Refs. 7 and 43, were fully structurally optimised. Compositional variations, by Al substituting Cr on the metallic sublattice, were considered for 9 different concentrations (Al content x = 0, 0.125, 0.25, 0.375, 0.5, 0.625, 0.75, 0.875, and 1). Three species, Al, Cr spin up, and Cr spin down, were distributed on the metallic sublattice following the special quasi-random structures (SQS) approach[44,45] to simulate the paramagnetic state of Al_2O_3 –Cr_2O_3 solid solution (i.e., treating it as a quasi-ternary syste m), an approach successfully applied before to e.g. $Cr_{1-x}Al_xN$ System.[46] The short range order parameters were optimized for pairs up to the fifth coordination shell. The resulting total magnetic moments were indeed close to zero μ_B as should be the case for the paramagnetic state.

The impact of point defects is studied using supercells including Frenkel pairs and Schottky defects. The former are constructed by shifting one Al, Cr, or O ion into an inherently unoccupied octahedral or tetrahedral interstitial lattice site for the B1-like and γ phases. For the α phase, the rearranged ion is placed only on vacant octahedral sites of the metallic sublattice. Schottky defects were created by randomly removing 2 metal and 3 oxygen atoms. These type of defects guarantee for the preservation of the overall charge neutrality preventing local electrically polar areas, hence an electrical disorder, which single point defects would evoke.

III. RESULTS AND DISCUSSION

A. Phase stability of perfect structures

The energy of formation per atom, E_f, is obtained from the total energy, E_{tot}, of the three crystallographic structures (α, γ, and B1-like) using

$$E_f = \frac{1}{80}\left(E_{tot} - 32\ (1-x)\ E_{Al} - 32\ x\ E_{Cr} - 48\ \frac{E_{O2}}{2}\right) \quad (1)$$

where E_{Al}, E_{Cr}, and E_{O2} are the formation energies of elements in their stable configurations fcc Al, bcc Cr, and O_2 molecule, respectively.

The α phase exhibits the lowest energy of formation over the entire composition range (Fig. 1(a)). For the boundary compositions x = 0 and x = 1, representing Cr_2O_3 and Al_2O_3, E_f equals -2.403 and -3.490 eV/atom, respectively. These values agree well with previously reported experimental and calculated data[49] of -2.384 and -3.494 eV/atom, respectively, and point out the higher overall chemical stability of Al_2O_3 in its hexagonal phase as compared with Cr_2O_3. For Al_2O_3, the γ phase (green diamonds in Fig. 1(a)) is more stable than the B1-like phase (red squares in Fig. 1(a)). With increasing Cr content the B1-like-modification becomes more stable than the γ phase, and already for x ≈ 0.85 both phases have nearly identical E_f values. The energy difference, $\Delta E_f^{B1-\gamma}$, between B1-like and γ is between -25 and +25 meV/atom for x ≥ 0.75, (open black circles in Fig. 1(b)). These values are comparable to k_BT (k_B Boltzmann constant, T temperature) at room temperature, and thus in the same range as vibrational excitations. At temperatures around 500 and 600 °C, a typical PVD substrate temperature for depositions of oxide coatings, k_BT equals to ~70 meV. Consequently, the energy difference of 25 meV/atom between these two phases, γ and B1-like, can easily be overcome by thermal excitations and hence both are expected to crystallize simultaneously during growth. For higher Cr concentrations, $\Delta E_f^{B1-\gamma}$ becomes increasingly larger, which is an indication for a B1-like preference over γ. This is in excellent agreement with experimental results showing that the B1-like phase fractions have first been detected for $(Al_xCr_{1-x})_2O_3$ coatings with increased Cr contents.[8] When

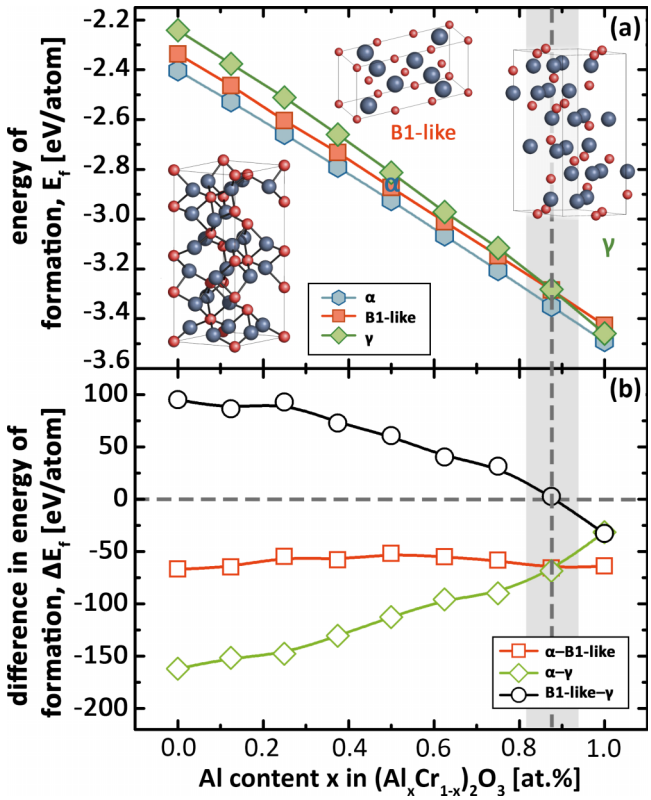

FIG. 1. (a) Energy of formation, E_f, of the corundum (blue hexagons), B1-like (red squares), and γ (green diamonds) solid solution of $(Al_xCr_{1-x})_2O_3$ plotted as a function of the Al content x. The transition between the preference for B1-like or γ as metastable phases, is marked by the shaded area. (b) Differences in E_f for α – B1-like (open red squares), α – γ (open green diamonds), and B1-like – γ (open black circles), respectively. Negative values indicate the preference of the first over the second one (e.g., negative values for α – γ indicate that α is preferred over γ) and vice-versa. The supercell illustrations are based on Refs. 47 and 48.

comparing the energy of formation between α and γ ($\Delta E_f^{\alpha\gamma}$, open green diamonds in Fig. 1(b)), the difference of ~-25 meV/atom steadily increases to more negative values, highlighting the preference of α over γ towards the Cr-rich side of the quasi-binary system. This is not the case for the difference between α and B1-like, $\Delta E_f^{\alpha B1}$, which is approximately -60±5 meV/atom independent of the chemical composition. However, thermal vibrations may also overcome this energy, hence a coexistence and/or competitive growth of these phases is conceivable, thus giving a possible explanation for the observation of a multi-phased microstructure.[50–52]

The mixing enthalpy, ΔH_{mix}, shown in Fig. 2 is calculated by

$$\Delta H_{mix} = E((Al_xCr_{1-x})_2O_3) - xE(Al_2O_3) - (1-x)E(Cr_2O_3) \quad (2)$$

with $E((Al_xCr_{1-x})_2O_3)$ being the total energy of the ternary supercell, and $E(Al_2O_3)$ and $E(Cr_2O_3)$ the total energy of the binary oxides, respectively. ΔH_{mix}, between Al_2O_3 and Cr_2O_3 is positive over the entire composition range for all three studied phases. Consequently, any $(Al_xCr_{1-x})_2O_3$ solid solution is supersaturated and experiences a thermodynamical driving force for decomposition into its stable constituents Al_2O_3 and Cr_2O_3.[53] The γ-type solid solution yields the highest ΔH_{mix}, with a maximum of approximately 40 meV/atom at x ~0.5. On the other hand, the B1-like solid solution yields the smallest ΔH_{mix}, with a maximum of 12 meV/atom at x ~0.6, and being about half of values for the γ phase. This is in excellent agreement with the previously reported mixing enthalpies of the B1 and corundum structures by Alling et al.[11] In general, the driving force for decomposition of $(Al_xCr_{1-x})_2O_3$ is much smaller than for many nitrides that are routinely synthesised using PVD as solid solutions. For example, rock-salt cubic $Ti_{1-x}Al_xN$, a prototype hard coating system, peaks x ~0.66[54–56] with a maximum value ΔH_{mix},~100 meV/atom. Despite this high driving force

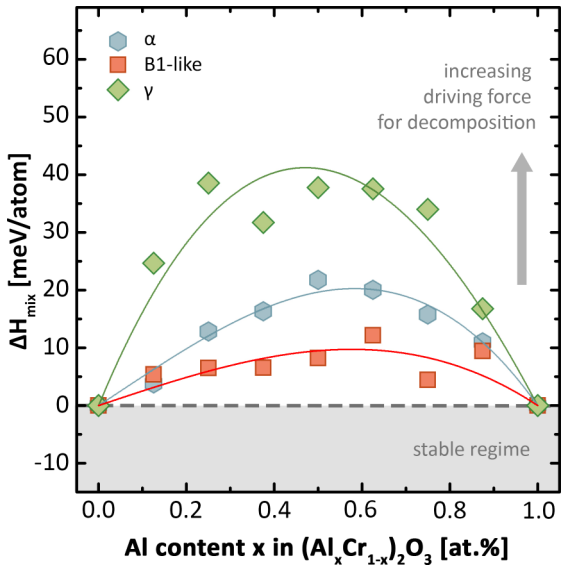

FIG. 2. Mixing enthalpy ΔH_{mix}, of the corundum (blue hexagons), B1-like (red squares), and γ (green diamonds) solid solution of $(Al_xCr_{1-x})_2O_3$ plotted as a function of the Al content x. The data are fitted with third order polynomial functions.

for decomposition, $Ti_{1-x}Al_xN$ can still be prepared using PVD as a cubic-structured single-phase solid solution, hence suggesting that the $(Al_xCr_{1-x})_2O_3$ supersaturated phases are not only realisable by PVD, but should be also more stable with respect to isostructural decomposition than, e.g., $Ti_{1-x}Al_xN$.

Based on the results presented in Figs. 1 and 2 we conclude that the corundum-type α-$(Al_xCr_{1-x})_2O_3$ is preferred over the metastable cubic phases in the entire composition range. Among these cubic phases (B1-like and γ), the B1-like structure is clearly energetically favoured with respect to the energy of formation, already for Cr contents above 15 at.% (1-x ≤ 0.85) of the metal sublattice. This is in agreement with equilibrium phase diagram showing that the corundum phase is the stable configuration of Al_2O_3, and suggesting a miscibility gap in the quasi-binary $(Al_xCr_{1-x})_2O_3$.[53,57]

Nevertheless, single-phase corundum-type $(Al_xCr_{1-x})_2O_3$ coatings can only be prepared by PVD at around or above 600 °C combined with Al contents x <0.5 or at lower temperatures for Cr contents above 70 at.% of the metal sublattice. On this account, some researchers have already reported on the effect of impurities[58] or interface and grain boundary energies[19,59] in order to examine phase stability and phase formation of Al_2O_3. Molecular dynamics simulations were employed to extensively study the impact of deposition temperature and bombardment on the stability of growing α and γ Al_2O_3.[60,61] This seems to be particularly appropriate when investigating PVD-deposited material systems where the incoming high energy atoms not only bring energy enhancing the surface ad atom mobility, but also may penetrate into the subsurface regions, hence resulting in far-from-equilibrium conditions. In the following we will therefore address the impact of point defects on phase stability in $(Al_xCr_{1-x})_2O_3$ with the aim to contribute to the ongoing scientific discussion on the puzzling discrepancy between experiments and theory.

B. Impact of point defects on the phase stability

The simplest point defects in bulk materials include vacancies, interstitials and anti-sites. All of these, however, change locally the anion-cation ratio, which in the case of ionic insulators poses a difficulty related to balancing the change.[26] To avoid this topic, we shall focus on defects which keep the number of anion and cation unaltered (Frenkel defects consisting of vacancy and interstitial pairs), or remove the whole formula unit (Schottky defects) hence maintaining the change neutrality of the overall system. Due to the complexity of the configurational space for various Al/Cr ratios

and defect arrangements, we restrict ourselves to only one industrially important chemical composition, $(Al_{0.7}Cr_{0.3})_2O_3$.

The energy of formation is a standard quantity for discussing the phase stability, as done in the previous section. We therefore first estimate the change of E_f and related phase preference, caused by the presence of Frenkel pairs and Schottky defects. The energy of formation was evaluated using Eq. (1). adjusted for the actual number of atoms in the defected supercell based on a perfect structure composed of 22 Al, 10 Cr, and 48 O atoms ($(Al_{0.69}Cr_{0.31})_2O_3$) being close to the experimentally aspired composition $(Al_{0.7}Cr_{0.3})_2O_3$. To better account for the statistical nature of defect formation, we set up different distributions of the defects. The Frenkel pairs were modelled by displacing an atom into a vacant position (either interstitial with respect to underlying perfect lattices, or vacant due to the construction of the oxide itself, e.g, the B1-like oxide with metal-to-non-metal ratio 2:3). Subsequently, the structural models were fully relaxed, and the final configurations were quantified by the distance between vacancy (before relaxation) and the interstitial atom (after the relaxation). In some cases, the relaxation led to a swap mechanism with another lattice atom, resulting in the original perfect structure again (in which two atoms swapped their places). Such configurations, as well as those in which the displaced atom relaxed back into its original position, were not further considered.

Changes in the energy of formation of $(Al_{0.69}Cr_{0.31})_2O_3$ caused by the generation of Al, Cr, or O Frenkel pairs are summarised in Fig. 3(a). The metal atom Frenkel pairs (e.g., an Al vacancy and an Al interstitial labelled as $V_{Al}Al_i$), result in increased (less negative) in E_f of the α, B1-like, and γ structures, whereof the least impact is observed for the latter. This increase of 49±21 meV/atom and 29±4 meV/atom for the α and the B1-like structures, respectively, in the case of $V_{Al}Al_i$, and of 67±5 meV/atom and 60±4 meV/atom for the α and the B1-like structures, respectively, in the case of $V_{Cr}Cr_i$, indicates stabilisation of the γ phase with respect to these two phases once the defects are present. Similarly, the O Frenkel pair strongly stabilises the cubic B1 structure. It can be therefore concluded, that all three types of Frenkel pair lead to a stabilisation of the cubic (γ or B1) phases with respect to the hexagonal α phase.

The effect of Schottky defects–with single metallic (i.e., vacancies at Al positions or Cr positions combined with vacancies at oxygen positions, $2V_{Al}3V_O$ and $2V_{Cr}3V_O$) or mixed metallic (i.e., one Al plus one Cr vacancy combined with three oxygen vacancies, $V_{Al}V_{Cr}3V_O$) species–is presented in Fig. 3(b). In this case, the energy of formation of all three phases becomes less negative in the presence of defects. While the Al Schottky defect keeps the relative phase stability between

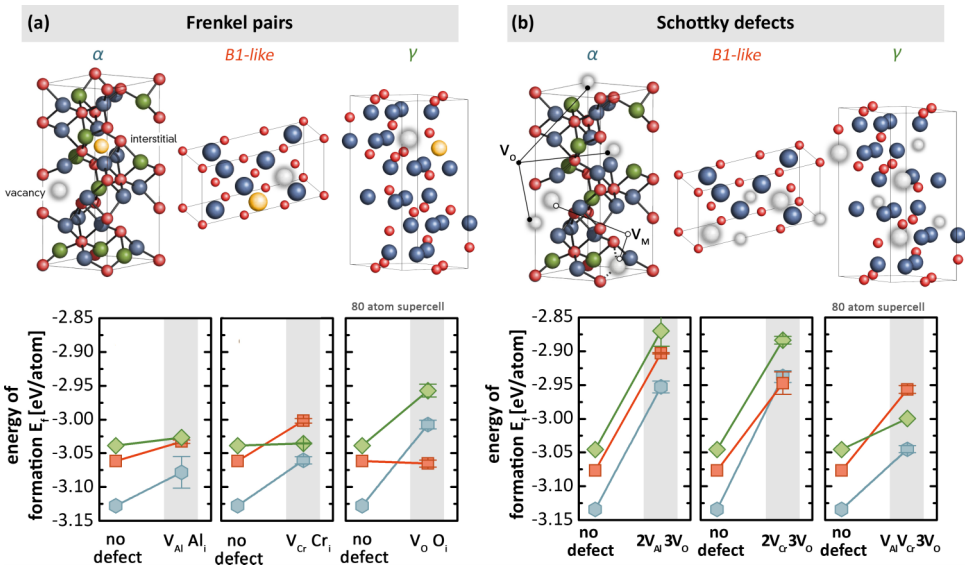

FIG. 3. Change in the energy of formation upon the generation of (a) one Frenkel defect and (b) one Schottky defect in α (blue hexagons), B1−like (red squares), and γ (green diamonds) solid solution $(Al_{0.69}Cr_{0.31})_2O_3$.

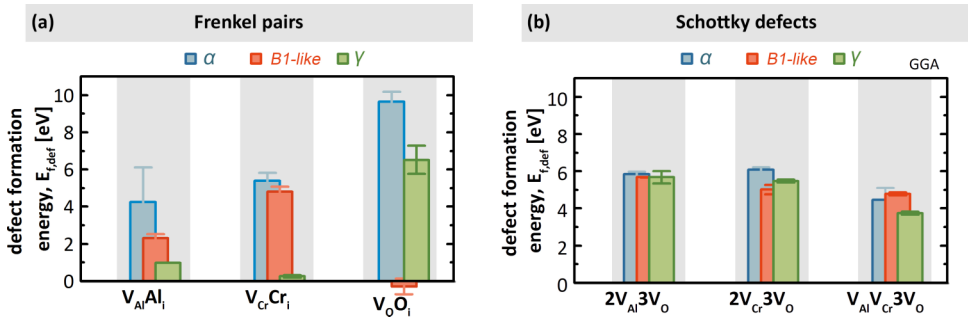

FIG. 4. Defect formation energy, $E_{f,def}$, per defect–(a) Frenkel pairs, and (b) Schottky defects for the α (blue), B1-like (red), and γ phase (green).

α, B1-like, and γ structures unchanged, the Cr Schottky defect leads to a strong preference of the B1-like phase. Interestingly, the mixed Al-Cr Schottky defect reduces E_f less than the single-specie defects, hence resulting in the most stable $(Al_xCr_{1-x})_2O_3$ containing a Schottky defect. Additionally, the mixed Schottky defect prefers the γ over the B1-like cubic structure.

C. Formation energies of point defects

The remaining question is, how energetically expensive it is to create the considered defects. Hence, we calculated the defect formation energies (Fig. 4) as

$$E_{f,def} = E_{t,def} - E_t \ (Frenkel\ defects) \tag{3}$$

$$E_{f,def} = E_{t,def} - (E_t - E_t(f.u.)) \ (Schottky\ defects) \tag{4}$$

where $E_{t,def}$ is the total energy of the supercell containing a specific defect type, and E_t is the total energy of the perfect crystal in the same supercell. E_t (f.u.) represents the chemical energy corresponding to atom forming the "formula unit" removed when creating a Schottky defect. In all cases, incorporated atoms were placed into lattice position demonstrating sufficient space. Positions with a smaller volume resulted in unrealistically high formation energies, and thus were excluded from the following discussion.

The calculated values are of the same order of magnitude as the literature data. For example, Lagerlöf and Grimes listed increasing formation energies of 4.87, 5.17, and 6.59 eV for oxygen Frenkel pairs, Schottky defects, and aluminium Frenkel pairs in corundum Al_2O_3[62] (cf. values for $V_{Al}Al_i$ and Schottky defects in Fig. 4.). On the other hand, Matsunaga et al. predicted using first principles plane-wave pseudopotential calculations, that Schottky defects are energetically favoured over anion and cation Frenkel pairs[31] in α-Al_2O_3, in agreement with previous work by Mohapatra and Kröger.[63] Similar findings were reported also by Corish and co-workers for α-Cr_2O_3.[64] Our calculations, on the other hand, show different ordering of the defects for all three here investigated structures. Moreover, in addition to the literature reports on binary oxides, the current case of $(Al,Cr)_2O_3$ presents a significant structural complexity (three types of Frenkel pairs, three types of Schottky defects). We therefore anticipate that results for individual Al_2O_3 and Cr_2O_3 compounds are directly not fully transferable to their solid solution $(Al,Cr)_2O_3$.

It is worth noting, that the cubic phases also yield Frenkel pair configurations with non-zero distance between the vacancy and the interstitial, but an almost zero change (increase or even decrease) of the energy of formation ($V_{Cr}Cr_i$ for the γ and V_OO_i for the B1-like phase). This points out that the current structural model (defected spinel for the γ phase and the ordered vacancies for the B1-like phase) are liable to structural modifications at almost no energy cost.

Comparing Figs. 4(a) and 4(b), one can see that for every structure, the lowest defect formation energy is obtained for some Frenkel-type defect, hence making them strongly preferred defect over the Schottky defects. The data in Fig. 4(a), in fact, visualise the same information as in Fig. 3(a) due to the fact that the number of atoms in the defect and perfect cells is the same. For example, the

almost zero $E_{f,def}$ of V_OO_i reflects the almost constant E_f upon introduction of O-Frenkel pairs to the B1-like structure (Fig. 3). On the other hand, the data shown in Fig. 4(b) contain in addition to Fig. 3 the energy connected with the removal of the formula unit.

It is evident that this energy balance completely ignores the process of the defect creation. However, assuming that the incoming atoms have high enough kinetic energy to be implanted into the growing film and/or to create a defect. E_f is actually a measure of their stability, e.g., whether there is thermodynamic driving force for their recovery. Apparently, this recovery force is almost zero for the Frenkel pairs in the γ phase, while it is significantly non-zero for the metal Frenkel pairs in both the corundum and B1-like structures. The recovery process includes short range diffusion, causing local rearrangements and distortions, which may lead to a local destruction of the crystal structure and amorphisation, as demonstrated by the molecular dynamics studies of Houska.[60,61] On the other hand, the γ phase is able to accept the Frenkel pairs at almost no energy cost, and hence is able to maintain crystalline even in their presence, which is unavoidable during the PVD process.

IV. CONCLUSIONS

In this *ab initio* study we propose that the point defects–unavoidably present in the material, especially when prepared by physical vapour deposition processes–contribute towards stabilising the cubic phases at the expense of the thermodynamically stable hexagonal structure of $(Al_{0.69}Cr_{0.31})_2O_3$.

Three experimentally relevant structures (regarding cathodic arc evaporation), corundum-type α, defect-spinel γ, and the recently introduced B1-like modification, were investigated in detail for their energy of formation, E_f. Our results clearly show that the α phase is the most stable structure independent of the Al content x of defect-free $(Al_xCr_{1-x})_2O_3$ solid solutions. The difference between α and B1-like is rather constant over the whole compositional range, whereas between α and γ the energy difference continuously decreases with increasing Al content. Only for Al-rich compositions with more than ~85 at.% Al on the metal sublattice, the metastable γ phase is energetically favoured over the B1-like phase. Furthermore, the mixing enthalpy curves suggest that the quasi-binary $(Al_xCr_{1-x})_2O_3$ system does exhibit miscibility gap.

Energetics of Frenkel pairs and Schottky defects in $(Al_{0.69}Cr_{0.31})_2O_3$ were analysed revealing that metal Frenkel pairs are stabilising the cubic modifications, bringing them energetically close to the α phase. We envision that this, together with almost zero Frenkel defect formation energies in the γ phase, leads to competitive growth of the PVD oxide films, amorphisation of the α phase, and/or stabilisation of the cubic phases at low growth temperatures.

ACKNOWLEDGMENTS

The financial support by the Austrian Federal Ministry of Economy, Family and Youth and the National Foundation for Research, Technology and Development is gratefully acknowledged. We also thank the financial support of Plansee Composite Materials GmbH and Oerlikon Balzers, Oerlikon Coating Solutions AG. The computational results presented have been achieved using the Vienna Scientific Cluster (VSC). Access to computing and storage facilities owned by parties and projects contributing to the National Grid Infrastructure MetaCentrum, provided under the programme "Projects of Large Infrastructure for Research, Development, and Innovations" (LM2010005), is greatly appreciated.

[1] K. Bobzin, N. Bagcivan, A. Reinholdt, and M. Ewering, Surf. Coatings Technol. **205**, 1444 (2010).
[2] S.E. Cordes, CIRP J. Manuf. Sci. Technol. **5**, 20 (2012).
[3] P. Eklund, M. Sridharan, M. Sillassen, and J. Bøttiger, Thin Solid Films **516**, 7447 (2008).
[4] J.M. Andersson, Z. Czigány, P. Jin, and U. Helmersson, J. Vac. Sci. Technol. A Vacuum, Surfaces, Film. **22**, 117 (2004).
[5] J. Ramm, M. Ante, T. Bachmann, B. Widrig, H. Brändle, and M. Döbeli, Surf. Coatings Technol. **202**, 876 (2007).
[6] J. Ramm, A. Neels, B. Widrig, M. Döbeli, L.D.A. Vieira, A. Dommann, and H. Rudigier, Surf. Coatings Technol. **205**, 1356 (2010).
[7] A. Khatibi, J. Palisaitis, C. Höglund, A. Eriksson, P.O.Å. Persson, J. Jensen, J. Birch, P. Eklund, and L. Hultman, Thin Solid Films **519**, 2426 (2011).

[8] A. Khatibi, J. Lu, J. Jensen, P. Eklund, and L. Hultman, Surf. Coatings Technol. **206**, 3216 (2012).
[9] H. Najafi, A. Karimi, P. Dessarzin, and M. Morstein, Surf. Coatings Technol. **214**, 46 (2013).
[10] A. Khatibi, A. Genvad, E. Go, E. Göthelid, J. Jensen, P. Eklund, and L. Hultman, Acta Mater. **61**, 4811 (2013).
[11] B. Alling, A. Khatibi, S.I. Simak, P. Eklund, and L. Hultman, J. Vac. Sci. Technol. A Vacuum, Surfaces, Film. **31**, 030602 (2013).
[12] I. Petrov, P.B. Barna, L. Hultman, J.E.E. Greene, and I. Introduction, J. Vac. Sci. Technol. A Vacuum, Surfaces, Film. **21**, S117 (2003).
[13] J. Ramm, M. Ante, H. Brändle, A. Neels, A. Dommann, and M. Döbeli, Adv. Eng. Mater. **9**, 604 (2007).
[14] B.K. Tay, Z.W. Zhao, and D.H.C. Chua, Mater. Sci. Eng. R Reports **52**, 1 (2006).
[15] W. Ensinger, Nucl. Instruments Methods Phys. Res. Sect. B Beam Interact. with Mater. Atoms **127-128**, 796 (1997).
[16] W. Ensinger, Surf. Coatings Technol. **80**, 35 (1996).
[17] D.M. Mattox, J. Vac. Sci. Technol. A Vacuum, Surfaces, Film. **7**, 1105 (1989).
[18] D.E. Ashenford, F. Long, W.E. Hagston, B. Lunn, and A. Matthews, Surf. Coatings Technol. **116-119**, 699 (1999).
[19] D. Music, F. Nahif, K. Sarakinos, N. Friederichsen, and J.M. Schneider, Appl. Phys. Lett. **98**, 111908 (2011).
[20] H. Najafi, A. Karimi, P. Dessarzin, and M. Morstein, Thin Solid Films **520**, 1597 (2011).
[21] H. Najafi, A. Karimi, E. Oveisi, and M. Morstein, Thin Solid Films **572**, 176 (2014).
[22] R. Godby, M. Schlüter, and L. Sham, Phys. Rev. Lett. **56**, 2415 (1986).
[23] P. Rinke, A. Qteish, J. Neugebauer, and M. Scheffler, Phys. Status Solidi **245**, 929 (2008).
[24] C. Loschen, J. Carrasco, K.M. Neyman, and F. Illas, Phys. Rev. B **75**, 035115 (2007).
[25] A. Janotti, J.B. Varley, P. Rinke, N. Umezawa, G. Kresse, and C.G. Van de Walle, Phys. Rev. B **81**, 085212 (2010).
[26] C. Freysoldt, B. Grabowski, T. Hickel, J. Neugebauer, G. Kresse, A. Janotti, and C.G. Van de Walle, Rev. Mod. Phys. **86**, 253 (2014).
[27] V.I. Anisimov, J. Zaanen, and O.K. Andersen, Phys. Rev. B **44**, 943 (1991).
[28] V.I. Anisimov, F. Aryasetiawan, and A.I. Lichtenstein, J. Phys. Condens. Matter **9**, 767 (1997).
[29] A. V Krukau, O.A. Vydrov, A.F. Izmaylov, and G.E. Scuseria, J. Chem. Phys. **125**, 224106 (2006).
[30] J. Heyd, G.E. Scuseria, and M. Ernzerhof, J. Chem. Phys. **118**, 8207 (2003).
[31] K. Matsunaga, T. Tanaka, T. Yamamoto, and Y. Ikuhara, Phys. Rev. B **68**, 085110 (2003).
[32] K.J.W. Atkinson, R.W. Grimes, M.R. Levy, Z.L. Coull, and T. English, J. Eur. Ceram. Soc. **23**, 3059 (2003).
[33] J.R. Weber, A. Janotti, and C.G. Van de Walle, Microelectron. Eng. **86**, 1756 (2009).
[34] J.R. Weber, A. Janotti, and C.G. Van de Walle, J. Appl. Phys. **109**, 033715 (2011).
[35] M. Choi, A. Janotti, and C.G. Van de Walle, J. Appl. Phys. **113**, 044501 (2013).
[36] G. Kresse and J. Furthmu, Phys. Rev. B **54**, 11169 (1996).
[37] G. Kresse and D. Joubert, Phys. Rev. B **59**, 1758 (1999).
[38] J. Perdew, K. Burke, and M. Ernzerhof, Phys. Rev. Lett. **77**, 3865 (1996).
[39] I. Levin and D. Brandon, J. Am. Ceram. Soc. **81**, 1995 (2005).
[40] H. Pinto, R. Nieminen, and S. Elliott, Phys. Rev. B **70**, 125402 (2004).
[41] G. Gutiérrez, A. Taga, and B. Johansson, Phys. Rev. B **65**, 012101 (2001).
[42] F. Maglia, S. Gennari, and V. Buscaglia, J. Am. Ceram. Soc. **91**, 283 (2007).
[43] X.S. Du, S. Hak, T. Hibma, O.C. Rogojanu, and B. Struth, J. Cryst. Growth **293**, 228 (2006).
[44] S.-H. Wei, L. Ferreira, J. Bernard, and A. Zunger, Phys. Rev. B **42**, 9622 (1990).
[45] A. Zunger, S.-H. Wei, L.G. Ferreira, and J.E. Bernard, Phys. Rev. Lett. **65**, 353 (1990).
[46] L. Zhou, D. Holec, and P.H. Mayrhofer, J. Appl. Phys. **113**, 043511 (2013).
[47] K. Momma and F. Izumi, J. Appl. Crystallogr. **44**, 1272 (2011).
[48] G. Rollmann, A. Rohrbach, P. Entel, and J. Hafner, Phys. Rev. B **69**, 165107 (2004).
[49] G. Hautier, S.P. Ong, A. Jain, C.J. Moore, and G. Ceder, Phys. Rev. B **85**, 155208 (2012).
[50] M. Pohler, R. Franz, J. Ramm, P. Polcik, and C. Mitterer, Thin Solid Films **550**, 95 (2014).
[51] C.M. Koller, J. Ramm, S. Kolozsvári, F. Munnik, J. Paulitsch, and P.H. Mayrhofer, Scr. Mater. **97**, 49 (2015).
[52] V. Edlmayr, M. Pohler, I. Letofsky-Papst, and C. Mitterer, Thin Solid Films **534**, 373 (2013).
[53] A.H. Schultz and V.S. Stubican, J. Am. Ceram. Soc. **53**, 613 (1970).
[54] D. Holec, L. Zhou, R. Rachbauer, and P.H. Mayrhofer, J. Appl. Phys. **113**, 113510 (2013).
[55] D. Holec, R. Rachbauer, L. Chen, L. Wang, D. Luef, and P.H. Mayrhofer, Surf. Coat. Technol. **206**, 1698 (2011).
[56] B. Alling, M. Odén, L. Hultman, and I.A. Abrikosov, Appl. Phys. Lett. **95**, 181906 (2009).
[57] S.S. Kim and T.H. Sanders, J. Am. Ceram. Soc. **84**, 1881 (2004).
[58] E. Wallin, J.M. Andersson, M. Lattemann, U. Helmersson, and M., 3877 (2008).
[59] E. Wallin, J.M. Andersson, E.P. Münger, V. Chirita, and U. Helmersson, Phys. Rev. B **74**, 125409 (2006).
[60] J. Houska, Surf. Coatings Technol. **254**, 131 (2014).
[61] J. Houska, Surf. Coatings Technol. **235**, 333 (2013).
[62] R.W. Grimes and K.P.D. Lagerlof, Acta Metall. **46**, 5689 (1998).
[63] S.K. Mohapatra and F.A. Kröger, J. Am. Ceram. Soc. **61**, 106 (1978).
[64] J. Corish, J. Hennessy, and W.C. Mackrodt, **49**, 42 (1988).